ЖУРНАЛ СТРУКТУРНОЙ ХИМИИ

2009. Том 50, № 2 *Март – апрель* *С. 288 – 301*

UDC 544.726:549.08

PROTON ADSORPTION AND ACID-BASE PROPERTIES OF TUNISIAN ILLITES IN AQUEOUS SOLUTION

© 2009 **A. Kriaa[1,2]*, N. Hamdi[2], E. Srasra[2]**

[1]*Département de Chimie, Ecole Supérieure des Sciences et Techniques de Tunis, Rue Taha Hussein-Montfleury Tunis, Tunisia*
[2]*Unité matériaux, Technopole Borj Cedria, BP 95-2050 Hammam Lif, Tunisia*

Received September, 8, 2008

Suspensions of illite clay minerals samples of three different origins (American illite from Montana, It(Mo), Tunisian glauconite from Gafsa, It(Ga), and Tunisian illite — chlorite mixed layer from El Hamma, It(Ha)) were prepared. The Fourier Transform Infrared (FTIR) spectroscopy, X-ray Diffractometry (XRD), Electron Scanning Microscopy (SEM) and surface area measurements were used to characterize the three illite samples having different extent of isomorphic substitution. The layers have a permanent negative charge due to isomorphic substitutions and pH dependent charges on the surface hydroxyls on the edges. Surface speciation of these samples was investigated using continuous potentiometric titration and mass titration curves between pH 4 and 11 at 0.001, 0.01 and 0.1 M NaCl solutions at ambient temperature. The two methods revealed point of zero charge (PZC) of the amphoteric edges sites approximately similar to the purified samples, in the range ~7.5—8.5, ~8.2—8.7 and ~ 9.0—9.3 for It(Mo), It(Ha) and It(Ga), respectively. The PZCs of freshly prepared dispersions are higher than those reported in the literature indicating basic character of these samples (pH of equilibrium suspensions in distilled water were ~7.9—9). In the present study, the focus was on the surface charge characteristics. A simple SCM model approach is presented to explain the illite H^+ adsorption data. Surface weak acidic sites and surface ionization constants were calculated from titration data using regression methods. Sites with pKa_1^{int} values of 6—6.7; 5.4—5.8; 6.1—6.6 and sites at pKa_2^{int} values of 9.2—9.9; 10.2—10.4; 9.3—10 for It(Mo), It(Ga) and It(Ha), respectively, were assigned to amphoteric Al—OH and/or Fe—OH and Si—OH groups on the edges of illite samples.

K e y w o r d s: minerals, clays, illite, point of zero charge, potentiometric titration, surface ionization constants.

The study of electrochemical properties of the clay/water interface is important for understanding some surface charge characteristics in contact with aqueous solution, such as PZC (point of zero charge defined as the pH value where the net total particle charge is zero). This parameter may play a significant role in the adsorption mechanism of inorganic and organic species at the solid/solution interface. These properties govern the flotation, flocculation, coagulation and dispersion phenomena in suspension systems [1—3]. Furthermore, some authors [4] reported that the dispersion/flocculation behavior of soil colloids is closely regulated by the charge characteristic of these colloids. As a consequence, many methods have been developed so far for determining PZC. The often used are classical potentiometric titration technique (PT) and the mass titration method (MT).

On the other hand, the description of acid-base properties of different chemical systems is of major interest in many disciplines. In the case of clay minerals, from the point of view of their catalytic

* E-mail: kriaa1993@yahoo.fr

applications, they are important especially in soil chemistry [5]. Detailed knowledge of these properties may serve for fundamental chemical studies as well as for practical characterization of the systems behavior. Classical potentiometric titrations are usually used to characterize a certain numbers of acidic centers and to calculate surface constants ionization from titration data using graphical extrapolation methods. Another more general approach is used in the case of complex systems for which acidity constants are characterized by proton affinity distribution curves from potentiometric titration data. We can cite some excellent papers [5—7] where several types of proton interacting sites with different *pK* values were identified within experimental window (2—12). Concerning PAM and PAM-H montmorillonite samples, Jagiello et al., 1995 [5] showed by using proton affinity distribution that the acidity of these materials is related to the OH groups attached to differently coordinated aluminum cations. According to these authors, the peak at $pK \sim 8.5$ is assigned to clay sheets containing octahedrally coordinated aluminum and/or aluminum present in the pillar structure. Whereas the peak at $pK \sim 6.5$ can be attributed to the acidic sites related to the tetrahedrally coordinated aluminum.

The surface charge characterization of clay minerals, when permanent charges from isomorphic substitutions of ions in a clay crystal lattice and variable edge charges are present, is more complicated than that of metal oxides [8—10]. In this case, the intrinsic surface charge density (σ_{in}) can be defined as the sum of the net permanent (or structural) charge density (σ_0) and the net proton surface charge density (σ_H), *i.e.* $\sigma_{in} = (\sigma_0) + \sigma_H$ [11]. The term point of zero charge (PZC), defined as a unique pH where the net surface charge is zero, for amphoteric oxides bearing only pH dependent charges must be redefined in the case of clay minerals with both permanent and pH dependent charges. In this case, additional points of zero charge should be introduced [8].

The surface charge characterization of illite was not studied extensively. H^+ adsorption was studied in the course of characterization of metal oxide (hydroxide) surfaces which carry only surface hydroxyl groups [12—14]. It is evident that there are remarkable differences between the protonation-deprotonation behaviors of mineral oxides and complex clay minerals. The difference is due to the fact that H^+ adsorption curves at different ionic strengths have a common intersection point which is the point of zero charge, whereas for illite and complex clay minerals the behavior seems to be different. In some investigations dealing with the surface charge characterization of Na^+-illite and several soils [15], the absence of intersection point in the pH range from 4 to 10 was observed and the curves had a very low slope near neutral pH. The absence of a crossing point was also reported for montmorillonitic samples [8, 10].

According to some authors [2], illite particles carry two types of electric charge: a variable (pH-dependent) charge (on the edges) resulting from proton adsorption-desorption reactions on surface hydroxyl groups and a permanent negative charge on the face resulting from isomorphous substitutions of Al^{3+} for Si^{4+} within the clay structure. Surface hydroxyl groups are located at the particle edges (10% of total surface area) and charges arise from the breaking of Al—O and Si—O bonds resulting in amphoteric Al—OH and Si—OH surface functional groups. These surface hydroxyls can be protonated or deprotonated depending on the pH of dispersion and the PZC of the edge of the clay particles. Moreover, Keren and Sparks, 1995 [3] reported that the most reactive surface functional group on the edge surfaces is the hydroxyl available on the periphery of the clay mineral. This functional group is associated with the structural cations Al^{3+} and Si^{4+} which are located in octahedral and tetrahedral sheets, respectively.

Concerning PZC values of illite clay minerals, we can observe a considerable variability of published experimental data. The values vary from 2.5 to ~7.5—8 [1—3, 15—17]. This disagreement can be attributed to differences in the origin of samples, to data treatment for determining PZC, and to different models used to interpret experimental data. It is evident that such variability had a direct influence on the determination of PZC value and, as a consequence, prevents comparisons and generalisations of published results for illite samples. Some successful studies dealing with aqueous illite surface, in order to elucidate its acid-base properties [17, 18] and its adsorptive properties [19], have been conducted but only few publications dealing with H^+ adsorption at different pH and ionic strengths appeared in the literature. Furthermore, there is a lack of papers dealing with the correlation between mineralogical compositions of illite clay minerals with the shifting of PZC values. In this pa-

per, in order to evaluate PZCs of illitic samples, we have used, in addition to fast titration technique, the mass titration method described by some authors [10, 20]. In this method, a limiting pH value is determined by increasing mass fractions of clay mineral (pH reaches a constant value after each addition of the mineral).

The present study was conducted (1) to evaluate surface charge characteristics and determine the point of zero charge by potentiometric and mass titration of illitic samples with different chemical compositions and (2) to propose a simple model approach for our illite samples in order to provide better understanding of H^+ adsorption data. For each illite sample, the total number of surface sites density and, consequently, the surface ionisation constants were calculated using regression methods.

MATERIALS AND METHODS CLAYS

The solid samples were obtained from three sources: (1) an American illite sample from Montana (USA) (light green color specimen); (2) an illite sample (glauconite) from Gafsa, in south Tunisia (dark green color specimen); and (3) an illite-chlorite mixed-layer sample from El Hamma, south Tunisia (reddish color specimen) (hereafter abbreviated as It(Mo), It(Ga) and It(Ha), respectively). The clay fraction (particle size < 2 micrometers) was purified by classical methods [21], using 1M NaCl solution. After washing, sedimentation and dialysis, the fine clean sediment was freeze-dried.

X-ray diffraction. X-ray diffractograms were recorded using a ″PANalytical X′Pert High Score Plus″ diffractometer with CuK_α filtered radiation in the 2θ range of 3—40° at a scanning rate of 2°/min. The diffractograms of oriented plate were obtained by sedimentation on slides. This procedure makes it possible to follow the periodicity of the stratification of the layers, with (d_{001}) being the reflection for which the identification is based.

FTIR Spectrometry. The infrared spectra were carried out using a Nicolet spectrophotometer, model 560. The samples were used in the pellet form containing 2 mg clay mixed with 200 mg of KBr. Scan time was 3 min for each spectrum.

Electron scanning microscopy. The micrographs were obtained on a scanning electron microscope (FEI, Quanta 2000), in order to analyze the external morphology of the solid samples.

Cation exchange capacities (CEC) and specific surface areas (SSA). CEC was determined by the method of copper ethylenediamine $(EDA)_2CuCl_2$ complex [22], and specific surface area was determined by nitrogen gas adsorption at 77 K after outgassing at 120 °C under helium gas, using a ″Quantachrome-Autosorb 1″ sorptiometer.

PZC determination by fast titration. Potentiometric titrations of the illitic samples were conducted in a reactor pyrex cell, microburette with very fine tip and a HI 9321 Microprocessor pH meter (Hanna Instruments) having combination electrode calibrated with two commercial pH buffers at ambient temperature and aerated medium.

The isotherms of proton adsorption curves at different salt concentrations were used to measure the proton adsorption or proton charge. The experimental method employed was similar to that used by Boisset, 1984 [23] for ″alumine, hematite and rutile″. 30 ml background electrolyte (NaCl) solution (0.1, 0.01, and 0.001 M) containing 0.05 g sample was equilibrated for 15 min with continuous stirring in order to reach an equilibrium pH value. Following equilibration at ambient temperature, 2 ml of 0.1 M HCl were added and the suspension was further agitated for 15 min. The new pH value of the suspension was recorded and then it was titrated by 0.2 ml of 0.05 M NaOH delivered by the microburette. After each addition of base, the suspension was equilibrated for 2 min with constant stirring; at the end of these 2 min period the changes were lesser than 0.03 pH units per minute.

All the experiments were carried out according to a continuous potentiometric titration and performed at least in duplicate to confirm the results [24]. On the average, percentage error (surface charge density) between the duplicates was less than 2 %. The blank titrations were also performed with similar solutions but without adding the solid sample.

Potentiometric titration curves. The proton adsorption or proton surface charge density σ_H (mol/m^2), determined from potentiometric titration was calculated as the difference between total amounts of H^+ or (OH^-) added to the dispersion and that required to bring a blank solution of the same NaCl concentration to the same pH [25].

$$\sigma_H(\mathrm{mol/m^2}) = \frac{V}{m} S \left\{ ([H^+]_b - [H^+]_s) - \left(\frac{K_w}{[H^+]_b} - \frac{K_w}{[H^+]_s} \right) \right\}, \quad (1)$$

where V is the volume of electrolyte solution equilibrated with illite sample (30 ml); $[H^+]$ is the solution proton concentration (mol/l); K_w is the dissociation product of water (10^{-14}) and the subscripts s and b refer to sample and blank solutions, respectively; m is the mass of sample used (0.05 g); S is the specific surface area (m^2/g).

Accuracy estimation: Based on the calibration titration and on the readings of the electrode potentials, the uncertainty in the measured pH was estimated to be ±0.1.

Regarding our potentiometric titration experiments, it is important to note that fast equilibration (rapid pH stability) was observed for the successive increments of NaOH. This is a useful observation because it permits to perform adsorption in a relatively short time. This observed fast equilibration can be understood as a result of reactions (adsorption or desorption) between protons and hydroxylated surface sites which are known to be very fast. Avena et al., 1998 [10] (see references therein), commented that the data reported by other authors indicated that proton adsorption reactions on FeOOH and silica – alumina were in the order of milliseconds.

PZC determination by mass titration. The mass titration method [10, 20] was used to determine the pH where $\sigma_H = 0$. Our experimental mass titration curves were obtained under the same conditions as potentiometric titration (aerated medium) by waiting until pH drift yields a steady value. Each addition was 0.05 g of the dry illite sample to 30 ml of NaCl solution at a given ionic strength $I = 0.01$ M. After each solid addition, the pH was recorded and, when equilibration was achieved, a new amount of sample was added to produce a new pH change. This procedure was repeated with a different initial pH until a pH was found where no pH change occurs with the addition of more sample. This is pH where proton adsorption is zero (PZC).

CHARACTERIZATION OF CLAY SAMPLES

X-ray patterns. The specimens after different treatments were studied by X-ray diffraction technique. In this procedure, an oriented specimen was prepared on glass microscope slides. The samples were successively subjected to different treatments not only to characterize the clay specimens but to identify the presence of interstratified or mixed other clay minerals:

i) Normal at ambient temperature (N);

ii) Saturated with ethylene glycol (EG-treatment) (G);

iii) Heating at 550 °C (H).

The diffractograms of the three illite samples are shown in Fig. 1 (patterns *a*, *b* and *c* correspond to It(Mo), It(Ga) and It(Ha), respectively).

In the patterns of the air-dried oriented samples of pure It(Mo) and pure It(Ga) (N), the basal reflections of illite appear along with an irrational series of reflections: $d_{(001)}$ reflection at 10.01 Å, $d_{(002)}$ at 5.01 Å and $d_{(003)}$ at 3.31 Å for It(Mo); and $d_{(001)}$ reflection at 10.10 Å, $d_{(002)}$ at 5.00 Å and $d_{(003)}$ at 3.32 Å for It(Ga). The XRD patterns of the EG-treated and heated specimens (H) at 550 °C were included in Fig. 1 in order to detect minimal changes. After EG-treatment (G) the illite basal reflections do not show significant changes for the two illite samples.

The XRD patterns of It-chlorite mixed layer It(Ha) show, in addition to peaks of illite at 9.97 Å, 4.98 Å and 3.31 Å, another series of reflections: $d_{(001)}$ reflection at 14.35 Å, $d_{(002)}$ at 7.13 Å and $d_{(003)}$ at 4.72 Å corresponding to chlorite clay mineral. After EG-treatment and heating specimens for 2 hours at 550 °C, the peaks at 7.06 Å and 4.72 Å did not disappear indicating the presence of chlorite mineral in illite. The peak surfaces of the d_{001} reflections of illite and chlorite were determined using a ′PANalytical X′Pert High Score Plus′ software. The amount of chlorite mineral in It(Ha) was estimated to be 20 %.

FTIR spectroscopy. FTIR was employed to characterize the illitic clay minerals; the resulting spectra in the range 4000—400 cm^{-1} are presented in Fig. 2. Sharp absorption bands at 1640 and 3400 cm^{-1} are, respectively, O—H bending and stretching bands of adsorbed water. The bands at

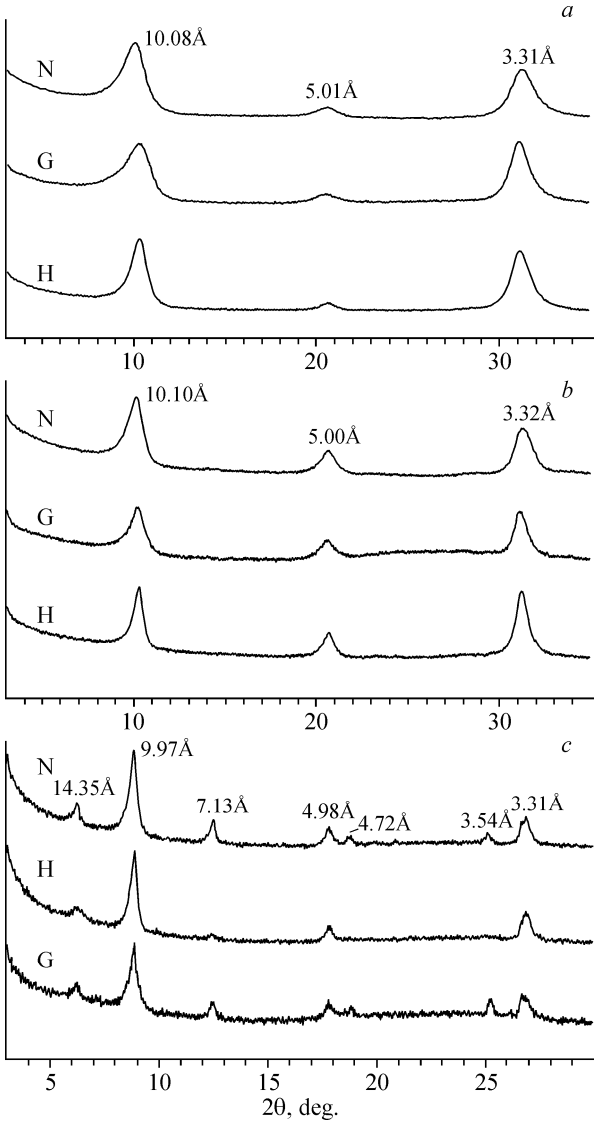

Fig. 1 (*left*). XRD patterns of oriented purified clay samples: *a* — It(Mo), *b* — It(Ga), *c* — It(Ha). N: Normal; H: heated at 550 °C; G: saturated by ethylene glycol

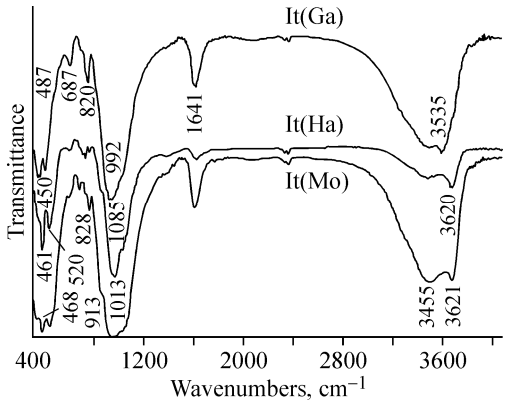

Fig. 2 (*right*). FTIR spectra of three illite samples studied

3620 cm^{-1} are Al_2OH stretching bands. The bands centered at 1085 and 1013 cm^{-1} for It(Mo) and It(Ha), respectively, are attributed to the presence of Si—O bonds [26]. In the case of It(Ga) sample, the band at 992 cm^{-1} is, probably, a Si—O stretch that is affected by Fe substitution. The shift of the bands from 1085 to 992 cm^{-1} with the increase in the content of Fe shows an increased association between SiOH and FeOH groups on the surface of It(Ga).

Electron Scan Microscopy. The scanning electron micrographs of three illite samples are shown in Fig. 3. The images reveal illite particles appearing as thin flakes; because of weaker interlayer bonds the particles are not as morphologically distinct.

Chemical analysis and structural formulas. The chemical analysis of purified illite samples is given in Table 1. The following can be concluded from the data:

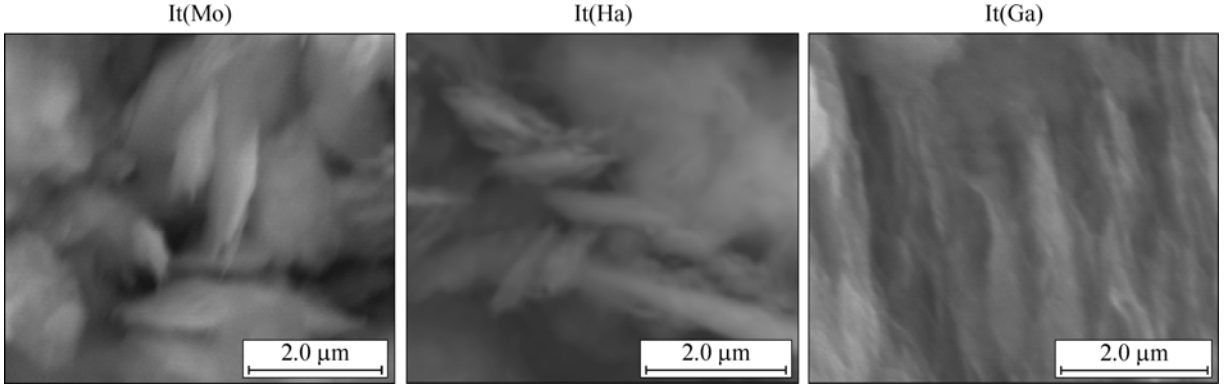

Fig. 3. Scanning electron micrographs of three illite samples studied

Table 1

Chemical composition of purified illite samples

Weight, %	SiO_2	Al_2O_3	Fe_2O_3	MgO	Na_2O	K_2O	CaO	Ignition loss
It(Mo)	50.24	24.38	5.58	2.13	1.21	9.39	0.05	7.53
It(Ga)	53.34	3.41	24.98	4.04	0.5	7.58	0.19	7
It(Ha)	53.42	15.82	9.44	3.49	2.08	7.04	0.89	8.05

Table 2

CEC cationic exchange capacity and SSA specific surface area values of It(Mo), It(Ga) *and* It(Ha)

Specimen	CEC (meq/100 g)	S_{BET} (m^2/g)	pH*
It(Mo)	27	45	7.9
It(Ga)	24	60	9.5
It(Ha)	34	51	8.2

* pH of liquor obtained after suspension of solid samples in distilled water. The solid/liquid ratio of the mixtures was 1.66 (g/l).

Comparatively to American illite It(Mo), the Tunisian glauconite It(Ga) contains a higher amount of Fe_2O_3 and lower Al_2O_3. One can notice that the three samples contain a high amount of K indicating that all samples are illitic clay minerals.

The average structural formulas of the purified It(Mo) and It(Ga) samples are:

$$\text{It(Mo): } K_{1.64}Ca_{0.01}Na_{0.32}\,[Si_{6.89}Al_{1.11}]^{IV}[Al_{2.82}Fe_{0.57}Mg_{0.44}]^{VI}\,O_{20}\,(OH)_4,$$

$$\text{It(Ga): } K_{1.40}Ca_{0.03}Na_{0.15}\,[Si_{7.70}Al_{0.3}]^{IV}[Al_{0.28}Fe_{2.71}Mg_{0.86}]^{VI}\,O_{20}\,(OH)_4.$$

The structural formula of It(Ha) has not been determined. The presence of chlorite mineral in its structure makes the formula more complicated.

It is seen from these formulas that illite samples used in this study present two types of substitutions (octahedral and tetrahedral). The charge per unit cell is 1.61 for It(Ga) and 1.98 for It(Mo). As can be noticed, the It(Ga) sample contains essentially Fe in the octahedral sheet, but in the It(Mo) sample, Al (III) occupies the octahedral sheet. Moreover, the tetrahedral substitution rate is more important for It(Mo) than for It(Ga).

Cation exchange capacity. The cationic exchange capacities (CEC) and the specific surface areas (SSA) for the three purified samples are summarized in Table 2. It appears that all CEC values are relatively lower of those reported for smectite clay minerals indicating that these solid samples belong to illite group. The S_{BET} values of these samples are close.

RESULTS AND DISCUSSION

Surface charge characteristics. Fig. 4, 5 and 6 show experimental isotherms of proton adsorption curves for It(Mo), It(Ga) and It(Ha) samples, respectively, dispersed in NaCl solutions of three different concentrations. First, one can observe for all studied samples that illite surface undergoes one protonation and one deprotonation reactions in the pH range 4—10. Unlike for It(Ga) and It(Ha), It(Mo) shows a slower adsorption at pH between 7 and 9 (gentle slope) that indicates a decreasing in protonation-deprotonation reactions. This could be due to (i) edge to face interactions between positively and negatively charged faces which would slow the protonation or deprotonation at hydroxylated sites on edges and (ii) CEC exchange reactions on the faces followed by a face to face aggregation that would decrease ion diffusion. This process is related to particle aggregation induced by protonation of the surface which was demonstrated by coagulation and rheologic studies [7, 8, 10].

On the other hand, our experimental titration curves demonstrate that the studied illite samples do not show a net crossing point in the proton adsorption curves differing from classical curves of pure simple oxides at various ionic strengths [14, 9]. In the case of our illite suspensions, the PZCs correspond to the pH where titration curves crossed with those of the corresponding blank solutions.

Some authors [10] reported that the absence of intersection point was attributed to a combined effect of both variable charges and permanent negative charge. It should be pointed out that the behavior of acid base titration curves of oxides is different from the behavior observed for complex clay minerals. In other words, the variations of $\sigma_H = f(\text{pH})$ suggests that the titration behavior of complex clay mineral such as illite may not be accurately represented by the contribution of the various con-

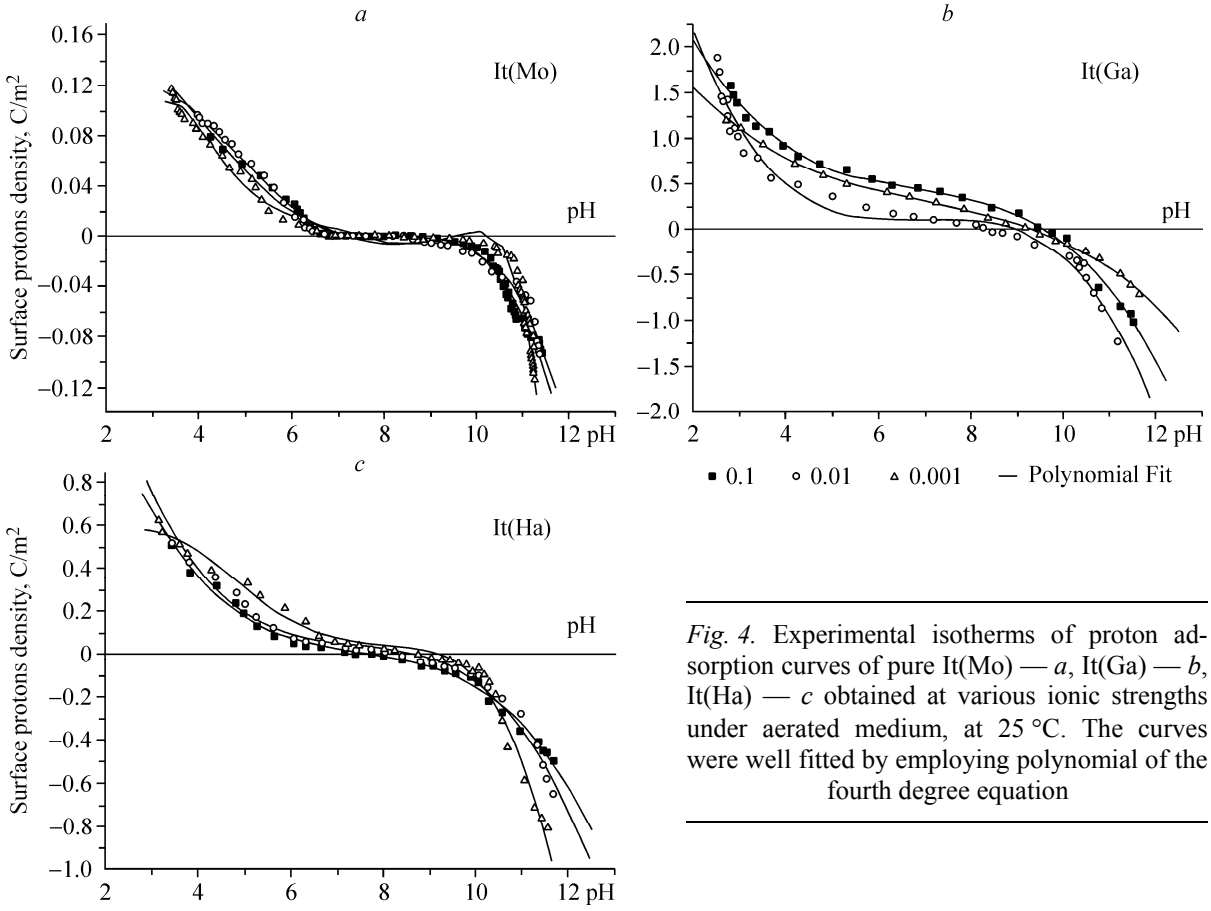

Fig. 4. Experimental isotherms of proton adsorption curves of pure It(Mo) — *a*, It(Ga) — *b*, It(Ha) — *c* obtained at various ionic strengths under aerated medium, at 25 °C. The curves were well fitted by employing polynomial of the fourth degree equation

stituents-oxides comprising the mineral (Al_2O_3, SiO_2, MgO, CaO, K_2O, *etc.*). A similar observation was reported in previous studies involving complex clay minerals and oxide minerals. For example, Lu and Smith, (1996) [32] (see references therein) compared surface properties of oxide and aluminosilicate minerals and determined that aluminol and/or silanol sites in aluminosilicates have markedly different surface properties than SiO_2 and Al_2O_3.

For complex clay minerals, many authors have found that the proton adsorption decreases as the electrolyte concentration increases (*e.g.* Avena and De Pauli, 1998 [10]; Tombacz and Szekeres, 2004 [8] for montmorillonite samples; Hendershot and Lavkulich, 1983 [15] for illite sample). In our case, we must emphasize that the studied illite samples presented proton adsorption *vs* pH curves typical of materials carrying mainly permanent or structural negative charges (see Fig. 4—6). In other words, our proton adsorption data exhibit unusual characteristics as compared to the ″classic″ curves usually obtained for oxides. This phenomenon has been already observed in the literature by some investigators [9, 12, 14].

The PZC values of illites samples are situated in pH ranges ~7.5—8.4; ~8.2—8.7 and ~9.1—9.3 for It(Mo), It(Ha) and It(Ga), respectively. It reveals that the presence of chlorite has no effect on the shifting of PZC value of It(Ha) toward higher pH. In this case, no experimental studies dealing with H^+ adsorption of chlorite were found in the literature. Our PZC values are in agreement with Hendershot and Lavkulich, 1983 [15] who found, for Na^+ illite, PZC value in the range ~7.5—8 in different NaCl solutions where *I* is varying from 0.002 M to 0.1 M. Comparatively to other experimental data published for illite, these values are somewhat higher. This result can be assigned to the basic character of our illite samples (the pH stability of the equilibrium suspensions in distilled water is in the range 7.9—9.5 with a solid / liquid ratio value of 1.66 g/l). Our results show that pure It(Ga) has a PZC value higher than It(Mo) and It(Ha). This is likely due to protonation—deprotonation of

Fe—OH groups on the edges of It(Ga). This behavior is similar to that observed for pure iron oxides where several experimental PZC values of different iron oxides are available in the literature. Parks, 1965 [27], reported that the isoelectric point of hematite is 9.03 determined in KNO_3 electrolyte solution at 21 °C; Mustapha et al., 2002 [28] found for $Fe(OH)_3$ a PZC value of 9 in NaCl electrolyte solution; Kosmulski, 2006 [29] reported for Goethite (FeOOH) a PZC value of 9.2 in 0.1M $NaNO_3$ electrolyte solution. Illes and Tombacz, 2004 [13], for magnetite (Fe_3O_4), found PZC value of 7.9 in different NaCl solutions.

On the other hand, some authors have noticed only one deprotonation reaction at the illite surface in the pH range 3—10 [17]. The same behavior was observed by Hussain et al., 1996 [1], by plotting zeta potential values *vs* pH; the Illite sample was negatively charged over pH range 2.5—11.

It must be stressed that our titration experiments were performed in aerated medium. The presence of CO_2 from air in the reactor can influence the shape of the titration curves in neutral to alkaline pH domain. In general, one can observe two forms of CO_2: free CO_2 absorbed from air and HCO_3^- adsorbed on the surface of the mineral. The presence of free CO_2 absorbed in water can be eliminated by subtracting the titration curves of blank solutions, which contain dissolved carbonate, from those of mineral suspension solution at the corresponding ionic strength (see equation (1) above). In the case of carbonate adsorbed at the mineral surface, the amount of the HCO_3^- is difficult to estimate because these species may be involved in equilibrium with the solid surface. However, we can consider that the amount of adsorbed HCO_3^- is negligible if we refer to pH uncertainty (±10 %) which is greater than the effect of CO_2.

We suggest that the differences in the shape of isotherms cited in the literature may be explained by the differences in sample chemical compositions and experimental conditions, such as equilibrium time, titration procedure and theoretical assumptions. Published results and conclusions concerning determination of point of zero charge and, as a consequence, surface reaction models of natural aqueous particles, may differ from case to case [17]. We think also that the major reason for the differences in the observed surface protonation is different ways in which the pH PZC was determined. As defined by the proton consumption equation (1), the titration curves measure a relative change in surface concentration and not the absolute concentration [25]. For illite clay mineral, we think that all different isotherms and plots should be reviewed if we want to compare them and we must define a common point of reference [8].

Mass titration curves. Mass titration data performed at a fixed NaCl concentration (I = 0.01 M) are shown in Fig. 5 for It(Mo), It(Ga) and It(Ha) samples, respectively. All the results concerning mass titration curves indicated the existence of a plateau on the pH *vs* added mass curve. We can notice that the pH gradually changes with the addition of the solid and asymptotically approaches a limiting value. The direction of the pH variation depends on the pH of the starting NaCl solution. Therefore, the pH where solid addition does not produce any change in the pH of the initial NaCl solution can be estimated by interpolation. The PZCs estimated this way are marked with arrows in Fig. 5. For the three illitic samples, their values were 8.5, 9.3 and 8.8 for It(Mo), It(Ga) and It(Ha) clay minerals, respectively, in 0.01 M NaCl solution. The differences observed in pH PZC values deter-

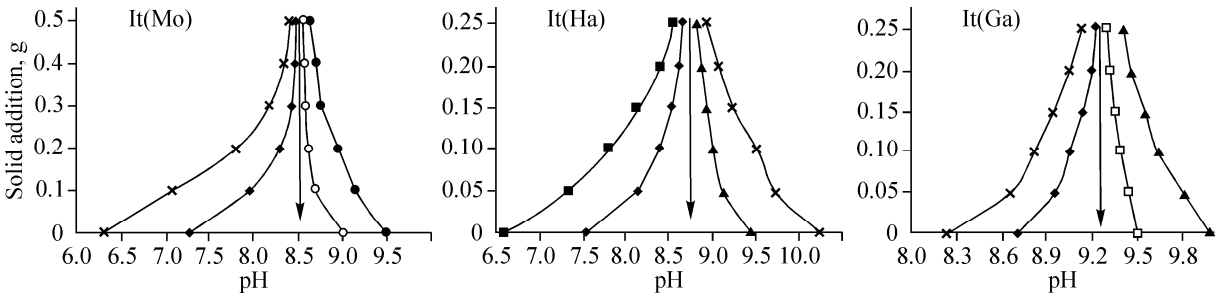

Fig. 5. Mass titration curves of pure illitic clay minerals at I = 0.01 M; each addition of the solid corresponds to 0.05 g of dry Illite sample

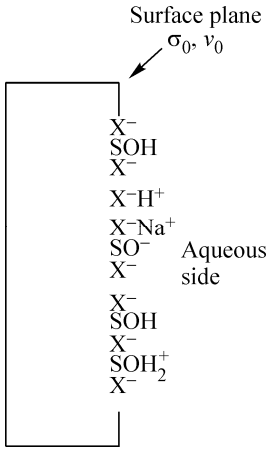

Fig. 6. Schematic representation of the clay surface

mined by potentiometric and mass titration methods may be due to specific adsorption of background ions on the illite surface in agreement with Noh and Schwarz, 1989 [20]. One may deduce that there is a very good agreement between acid-base potentiometric curves and mass titration curves.

A simple model approach using the principles of surface complexation modelling assuming the presence of permanent negative charges in the clay particles (on faces) and that H^+ or OH^- at low or high pH takes place on variable charge sites of illite edges. The model can be divided in two main parts: one represents the particle, the type and properties of reactive sites, the charge distribution in the particle, *etc.*, and the other represents the electrical double layer (EDL) that describes the charge distribution and potential decay on the aqueous side of the interface. The scheme of the clay particle is shown in Fig. 6. The structural charges are represented as a plane of negative charges inside the solid. At the surface, these charges are considered to express themselves as discrete sites X^- that can bind the cations present in the aqueous solution (Na^+ and H^+ in this case). The variable charges located at the edges of the particles are projected at the same surface as the sites X^-. That is to say, the distinction between the edge surface and the plate surface is neglected in the model. The permanent charges are in direct contact with the aqueous solution inducing proton and sodium binding to the surface. The Na^+/H^+ ion exchange process takes place on permanent charge sites of platy illite (on particle face) and protonation-deprotonation processes at edges in the negative electrostatic field emanating from the particle face.

The amount of permanent structural charges (σ_{str}) per unity of area (mol/m^2) in a particle is designated as N_{str}; and thus the charge density is:

$$\sigma_{str} = -FN_{str}, \tag{2}$$

with σ_{str} (C/m^2), N_{str} (mol/m^2) and F, the Faraday constant, (Coulomb/mol). The permanent charges can be surrounded either by H^+ or Na^+ adsorption on the X^- sites of the solid matrix. Hereafter, this type of surface sites is denoted as structural-charge surface sites or ″layer sites″. The reactions between the cations and the X^- sites are:

$$X^- + Na^+ \Leftrightarrow X^-Na^+ \quad K_{Na}^{int} \tag{3}$$

$$X^- + H^+ \Leftrightarrow X^-H^+ \quad K_{H}^{int} \tag{4}$$

with

$$K_{Na}^{int} = [X^-Na^+]/[X^-][Na^+]_s \exp(-F\Psi_0 / RT) \tag{5}$$

$$K_{H}^{int} = [X^-H^+]/[X^-][H^+]_s \exp(-F\Psi_0 / RT), \tag{6}$$

where $[X^-Na^+]$ and $[X^-H^+]$ denote the surface concentration (mol/m^2) of the X^- sites bounded to Na^+ and H^+, respectively. $[X^-]$ represents the permanent charges that have to be neutralized in the aqueous side of the double layer. $[Na^+]_s$ and $[H^+]_s$ are the bulk activity of Na^+ and H^+, respectively. Ψ_0 is the surface potential. The mass balance for X^- sites is expressed by:

$$N_{str} = N_X = [X^-] + [X^-Na^+] + [X^-H^+]. \tag{7}$$

The amount of permanent negative charges was estimated to be equal to the CEC of the samples [10] which means that the products FN_{str} (or σ_{str}) are 0.58 C/m^2, 0.386 C/m^2 and 0.64 C/m^2 for It(Mo), It(Ga) and It(Ha), respectively.

In addition to the permanent charge at the layers, the morphological structure of clays, also giving rise to a pH-dependent charge on the edge surface, must be considered. The strongly pH-dependent charge of the edges is due to adsorption of the potential-determining ions H^+ and OH^- as a function of the solution pH. The surface properties of the edge surface of the clay mineral are similar to those found for oxide surfaces [11, 30]. In our study, this type of surface sites is designated as variable-charge surface sites or ″edge sites″. The variable charge sites (Ns) were evaluated from fits of proton

adsorption data. The products *FN*s were set equal to 0.097 C/m^2, 0.15 C/m^2 and 0.39 C/m^2 for It(Mo), It(Ga) and It(Ha), respectively. The σ_{str} of It(Ga) is lower than that of It(Mo); this is due to the low rate of tetrahedral substitutions in It(Ga) (see structural formula) since for illite isomorphic substitutions take place mainly by replacing Si^{4+} by Al^{3+} ions in the tetrahedral sheets [10]. In addition to cation exchange reactions, the contribution of proton binding by variable charge site of edges should be mentioned. The chemical reactions on the edges are:

$$\left.\begin{aligned} \underline{\text{Al}}\text{—OH} + \text{H}^+ &\Leftrightarrow \underline{\text{Al}}\text{—OH}_2^- \\ \underline{\text{Fe}}\text{—OH} + \text{H}^+ &\Leftrightarrow \underline{\text{Fe}}\text{—OH}_2^- \end{aligned}\right\} \text{positive}$$

$$\left.\begin{aligned} \underline{\text{Al}}\text{—OH} + \text{OH}^- &\Leftrightarrow \underline{\text{Al}}\text{—O}^- + \text{H}_2\text{O} \\ \underline{\text{Si}}\text{—OH} + \text{OH}^- &\Leftrightarrow \underline{\text{Si}}\text{—O}^- + \text{H}_2\text{O} \end{aligned}\right\} \text{negative.}$$

The equilibrium constants Ka_1 and Ka_2 for the protonation and deprotonation reactions of edge sites account for the amphoteric character of the OH groups [11]. The variable charge sites are assumed to be equivalent to monoprotic weak acidic sites that can react according to

$$> \text{M}_\text{I}\text{OH}_2^+ \Leftrightarrow > \text{M}_\text{I}\text{OH} + \text{H}^+ \tag{8}$$

$$> \text{M}_\text{II}\text{OH} \Leftrightarrow > \text{M}_\text{II}\text{O}^- + \text{H}^+, \tag{9}$$

where >MOH, $> \text{M}_\text{I}\text{OH}_2^+$, and >MO$^-$ represent the corresponding surface hydroxyl groups of the edge surface, and Ka_1^{int} and Ka_2^{int} are intrinsic acidity constants. In this two sites — two *pKa* values model, the illite surface is considered as heterogeneous by assuming the existence of two types of surface sites (>M_IOH and >M_{II}OH), as shown in the equations (8) and (9), respectively. This hypothesis is deducted from analysis of data of proton adsorption isotherms for the different aqueous illite suspensions (see Fig. 4, 5 and 6). The weak acidic sites dissociate withing pH range 4—8, while weak basic sites dissociate at pH > 8. The intrinsic equilibrium constants for the different surface groups are expressed according equations (10) and (11).

$$K_1^{int} = [> \text{M}_\text{I}\text{OH}][\text{H}^+]_s / [> \text{M}_\text{I}\text{OH}_2^+] \exp(-F\Psi_0 / RT) \tag{10}$$

$$K_2^{int} = [> \text{M}_\text{II}\text{O}^-][\text{H}^+]_s / [> \text{M}_\text{II}\text{OH}] \exp(-F\Psi_0 / RT), \tag{11}$$

where [>M_IOH] and $[H^+]_s$ denote surface concentration and bulk activity of protons, respectively. F is the Faraday constant (Coulomb/mol), Ψ_0 is the surface potential (Volt), R and T are the gaz constant (cal/K mol) and temperature (K), respectively. The mass balance for variable charge site is given:

$$N_s = [> \text{M}_\text{I}\text{OH}_2^+] + [> \text{M}_\text{II}\text{O}^-] + [> \text{MOH}] \tag{12}$$

with [>MOH] = [>M_IOH] + [>M_{II}OH], where N_s is the surface density of variable charge sites.

Our approach to determine surface site densities and surface ionization constants (corresponding to reactions (8) and (9), respectively) is similar to that used by Huertas et al., 1998 [31]. Briefly, our experimental titration curves were fitted by least square regression analysis assuming the presence of two sites at the illite surface. From positive to negative surface charge, the illite surface undergoes two successive reactions: the reaction at the sites (θ_1) occurs from pH ~ 4.5—8 and it corresponds to the release of protons at weakly acidic sites; the sites (θ_2) start to deprotonate at pH ~ 8.5—9 forming negative complexes above pH = 9. These reactions occur at distinctly different pH, each site behaving as the only active site within certain pH range and, consequently, can be treated independently.

The intrinsic constants for the surface groups were calculated by extrapolating the linear regression curves *pKa vs* σ_H to zero surface charge. The total site density was estimated by extrapolating the sections of the titration curves to low or high pH values (Table 3).

The model used in our study assumes that the surface plane and the diffuse layer plane are separated by a region of constant capacitance, C_{St}, and that between the diffuse layer and the bulk of aqueous solution, the potential decay is according to Gouy-Chapman theory [10, 32, 33]. The surface charge σ_0 formed by ionized surface groups is localized on the surface plane with potential ψ_0. The specifically adsorbed electrolyte ions are assumed to lie in the Stern layer localized in the inner Hel-

T a b l e 3

Calculated surface site densities θ (μmol/m^2) *and intrinsic equilibrium constants for protonation and deprotonation surface reactions for* It(Mo), It(Ga) *and* It(Ha). *The capacitance* (*C*) *is in* F/m^2

It(Mo)							It(Ha)						
I(M)	θ_1	pKa_1^{int}	θ_2	pKa_2^{int}	θ_{total}	C at I = 0.1 M	I(M)	θ_1	pKa_1^{int}	θ_2	pKa_2^{int}	θ_{total}	C at I = 0.1 M
0.1	1.23	6.7	1.21	9.9	2.44	0.02	0.1	3.67	6.1	4.53	9.3	8.2	0.04
0.01	1.2	6.5	1.14	9.7	2.34		0.01	3.31	6.6	3.45	10	6.76	
0.001	1.56	6	1.63	9.2	3.19		0.001	5.08	6.1	7.2	9.9	12.28	

It(Ga)						
I(M)	θ_1	pKa_1^{int}	θ_2	pKa_2^{int}	θ_{total}	C at I = 0.1 M
0.1	10.6	5.8	8.09	10.4	18.69	0.06
0.01	9.74	5.6	2.66	10.4	12.4	
0.001	9.32	5.4	4.09	10.2	13.41	

mohltz plane with charge σ_{St} and potential ψ_{St}. The diffuse layer charge σ_d starts from the outer Helmohltz plane with potential ψ_d. The total interfacial capacitance C is expressed as $1/C = 1/C_{St} + 1/C_d$, where $C_{St} = \sigma_0/\psi_0 - \psi_{St}$ and $C_d = \sigma_0 + \sigma_{St}/\psi_{St} - \psi_d$ and ψ_d is the potential at the beginning of the diffuse layer.

The total interfacial capacitance C will be equal to C_{St} when $C_d \gg C_{St}$, *i.e.* at high ionic strength ($I \geq 0.1$ M). In our study, the total interface capacitance is given by the formula $d\sigma_0/d(pH \times 0.059) = C(F/g)$ [34]. The capacitances were obtained by graphical differentiation of curves at $I = 0.1$ M, (σ_0 *vs* pH; see Fig. 4, 5, 6 above) at the PZC using ORIGIN 6.1 software.

For It(Ga), the capacitance values are slightly higher comparatively to It(Mo) and It(Ha), due to their relative elevated surface charge density, likely emanating from sheets of octahedra with predominant iron. Our capacitance values are comparable to those published in the literature for montmorillonite [10]. Compared to illite of Hendershot and Lavkulich, 1983 [15], our capacitance values are slightly lower. Therefore, a lower capacitance value in illite suggests a lower influence of edges in determining the double layer structure. However, it should be realized that the assumption in the present model, *i.e.* that edges and faces conform the same surface plane, complicates the interpretation of the double layer structure. A more sophisticated model could perhaps improve some predictions but with consequent loss in simplicity.

The intrinsic equilibrium constants for the cation binding on permanent charged sites and for protonation and deprotonation of edge sites of It(Mo), It(Ga) and It(Ha), respectively, are summarised in Table 4.

Our results show that the affinity of our illite samples surface for cations is higher ($7.6 < \log K_H^{int} < 8.5$ and $8.3 < \log K_{Na}^{int} < 9$) of that reported for other complex clay minerals. For example, for Na^+ illite, Avena and De Pauli, 1998 [10], listed $\log K_H^{int} = 1.97$ and $\log K_{Na}^{int} = 2.28$. On the other

T a b l e 4

Parameters for the interfaces of illite samples in aqueous NaCl

Parameter	$\log K_H^{int}$	$\log K_{Na}^{int}$	pKa_1^{int}	pKa_2^{int}
It(Mo)	7.6	8.3	6—6.7	9.2—9.9
It(Ga)	8.8	9	5.4—5.8	10.2—10.4
It(Ha)	8.5	8.3	6.1—6.6	9.3—10.

hand, the overall surface ionization constants for protonation and deprotonation reactions of our illite edge sites are higher ($5.4 < pKa_1^{int} < 6.7$ and $9.2 < pKa_2^{int} < 10.4$) than those reported in literature for other complex clay minerals. For example, Lu and Smith, 1996 [35] listed $pKa_1^{int} = 4.77$—5.15 and $pKa_2^{int} = 7.63$—7.56 for glauconite without dissolution correction; Du et al., 1997 [17], by using two sites — two *pKa* model for illite from hebei China, found $pKa_1^{int} = 4.17$—4.44 and $pKa_2^{int} = 6.35$—7.74; Avena and De Pauli, 1998 [10] listed for illite $pKa_1^{int} = -3.90$ and $pKa_2^{int} = -7.60$. Our pKa^{int} values are not significantly different from those reported by Motta and Miranda, 1989 [36] for illite sample, under the assumption of the constant capacitance model; the two acid-base constants in the two neutral and alkaline pH regions were $pKa_1^{int} = 7.5$ and $pKa_2^{int} = 11.5$. This discrepancy might be due to the differences in the sources of the sample and/or in the experimental method, in agreement with Du et al., 1997 [17].

According to Janek and Lagaly, 2001 [7], the *pK* values 5—6 of weak acidic sites are very likely related to hydrated aluminum ions in solution (*pK* of $[Al(OH_2)_6]^{3+} = 4.8$). The slight high *pK* value may indicate that the hydrated Al^{3+} cations are attached to the clay mineral particles.

Glauconite sample It(Ga) reveals a higher number of surface site density than It(Mo) and It(Ha). The pKa_1^{int} values = 5.46—5.78 are slightly lower than It(Mo) and It(Ha). This decrease of the pKa_1^{int} values of It(Ga) comparatively to others illite samples may indicate the effect of hydrated Fe^{3+} cations, $[Fe(H_2O)_6]^{3+}$, which are known to be more acidic [7]. The slight changes in the pKa_1^{int} values between It(Mo) and It(Ga) samples indicate that similar but not fully identical species or groups are titrated. Very likely, there are two functional groups at the edges of It(Ga) surface: dominant Fe—OH and eventually Al—OH groups which are simultaneously protonated and deprotonated.

The pKa_2^{int} values of our illites samples (9.25—10.43) indicate that no precipitation reaction of aluminum hydroxide in form of surface precipitates can occur (*pK* values ~8). Janek and Lagaly (2001) [7] reported that the precipitation of magnesium hydroxide $Mg(OH)_2$ can occur at pH ~ 9.6. Consequently, our pKa_2^{int} for the illite samples may be influenced by coprecipitation with aluminum or iron ions in form of layered double hydroxides [37]. The relative high pKa_2^{int} values for It(Mo), It(Ga) and It(Ha) indicate the dissociation of silanol protons and/or silanol groups generated upon basic attack of Si—O—Si bonds.

It may be interesting to compare these results with the intrinsic equilibrium constants evaluated for oxide-water systems on the basis of different surface complexation models [38—40]. In these models, the proton dissociation reactions are formally described by reactions (8) and (9) cited above. The values of the intrinsic constants derived from the titration curves depend on the model chosen, *e.g.* constant capacitance model, triple layer model. Moreover, the experimental inaccuracy of the isotherms of proton adsorption did not lead to a unique set of data [32]. For alumina, Tombacz et al., 1995 [41] listed $\log K_1^{int} = 5.8 \pm 0.2$, $\log K_2^{int} = -10.2 \pm 0.2$, $pH_{PZC} = 8.01 \pm 0.1$, and for silica $\log K_1^{int} = -8.02 \pm 0.1$, $pH_{PZC} < 4.0$. For γ-Al_2O_3 in NaCl solution, Davis et al. (1978) [38] listed $Ka_1^{int} = 5.7$ and $Ka_2^{int} = 11.5$. Kummert and Stumm, (1980) [42] reported $pKa_1^{s}(int) = 7.4$ and $pKa_2^{s}(int) = 10.0$ for γ-Al_2O_3 in 0.1 M $NaClO_4$. The dissociation of silanol groups of illite is described by a relative pKa_2^{int} values 9.25—10.43 since we refer to *pK* value ~10 for orthosilicic acid in solution [7].

Therefore, we can conclude that acide-base properties of amphoteric edge sites of It(Mo) are situated between the surface OH bound to the pure Al_2O_3 and SiO_2 solid matrix, whereas for It(Ga), they are probably between the surface OH bound to the pure Fe_2O_3 and SiO_2 solid matrix. This conclusion based on the surface complexation modeling (SCM) of surface processes of illite is in good agreement with an empirical approach of the edge sites characterization, which assumes a weighted sum of the properties of pure Al—OH and Si—OH groups [8 (see references therein), 43]. The calculated intrinsic equilibrium constants show more details, since we can characterize the OH groups at edges having

PZC at pH ~ 7.5—8.4 for It(Mo) as less basic than the Al—OH and less acidic than Si—OH groups. Positive charge can develop only on the Al—OH sites of edges at pH below 7.5.

CONCLUSION

The following conclusions can be drawn from the above studies. The illite samples show proton adsorption *vs* pH curves typical of materials carrying mainly permanent negative charges and no net crossing point can be observed for several titration curves performed at different ionic strengths. The PZC values were in the range ~7.5—8.4, ~8.2—8.7 and ~9.1—9.3 for It(Mo), It(Ha) and It(Ga), respectively. Within the framework of the above experimental conditions, a good agreement between pH PZC values determined by potentiometric and mass titration curves of the studied illite samples was found. It reveals that the presence of chlorite in illite mixed layer has a noticeable effect on shifting PZC value of It(Ha) toward a high pH value.

The acid-base surface chemistry of illite resembled that described for other complex clay minerals in the literature. The pH of aqueous medium has two kinds of specific role, one is the high affinity of H^+ and Na^+ ions to neutralize the permanent negative charges of electric double layer on faces ($7.6 < \log K_H^{int} < 8.4$ and $8.3 < \log K_{Na}^{int} < 9$) and the other is providing chemical species (H^+ and OH^-) to the surface protolytic reactions on edge sites. For our illite samples, the surface ionization constant for protonation and deprotonation reactions of amphoteric edge site are higher than those reported in the literature and are situated between $5.4 < pKa_1^{int} < 6.7$ and $10.4 < pKa_2^{int} < 9.2$. From our study, since our analyses are limited to an experimental window 4—11, we cannot exclude the existence of certain acidic groups with *pKa* beyond this range related to complex structure of clay minerals. We think that this study should be completed by using proton binding affinity distribution method in order to detect new acidic centers that have not been identified by regression method.

REFERENCES

1. *Hussain S.A., Demicri S., Ozbayoglu G.J.* // Coll. Interf. Sci. – 1996. – **184**. – P. 535.
2. *Katari K., Tauxe L.* // Earth and Planetary Science Letters. – 2000. – **181**. – P. 489.
3. *Keren R., Sparks D.L.* // Soil Sci. Soc. Amer. J. – 1995. – **59**. – P. 430.
4. *Itami K., Fujitani H.* // Coll. Surf. A. – 2005. – **265**. – P. 55.
5. *Jagiello J., Bandosz T.J., Puteyra K., Schwarz J.A.* // J. Coll. Interf. Sci. – 1995. – **172**. – P. 341.
6. *Bandosz T.J., Jagiello J., Puteyra K., Schwarz J.A.* // J. Chem. Soc., Faraday Trans. – 1994. – **90**. – P. 3573.
7. *Janek M., Lagaly G.* // Appl. Clay Sci. – 2001. – **19**. – P. 121.
8. *Tombacz E., Szekeres M.* // Ibid. – 2004. – **27**. – P. 75.
9. *James R.O., Parks G.A.* Characterisation of aqueous colloids by their electrical double-layer and intrinsic surface chemical properties, in Surface and Colloids Science / Ed. E. Matijevic – N. Y.: Plenum Press, 1982. – **12**. – P. 119.
10. *Avena M.J., De Pauli C.P.* // J. Coll. Interf. Sci. – 1998. – **202**. – P. 195.
11. *Sposito G.* The surface chemistry of soils. – N. Y.: Oxford Univ. Press, 1982.
12. *Tombacz E., Szekeres M., Klumpp E.* // Langmuir. – 2001. – **17**. – P. 1420.
13. *Illes E., Tombacz E.* // Coll. Surf. A. – 2004. – **230**. – P. 99.
14. *Tombacz E., Szekeres M.* // Langmuir. – 2001. – **17**. – P. 1411.
15. *Hendershot W.H., Lavkulich L.M.* // Soil Sci. Soc. Amer. J. – 1983. – **47**. – P. 1252.
16. *Zhuang J., Yu G.R.* // Chemosphere. – 2002. – **49**. – P. 619.
17. *Du Q., Sun Z., Forsling W., Tang H.* // J. Coll. Interf. Sci. – 1997. – **187**. – P. 221.
18. *Liu W., Sun Z., Forsling W. et al.* // Ibid. – 1999. – **219**. – P. 48.
19. *Du Q., Sun Z., Forsling W., Tang H.* // Ibid. – 1997. – **187**. – P. 232.
20. *Noh J.S., Schwarz J.A.* // Ibid. – 1989. – **130**. – P. 157.
21. *Olphen V.* An Introduction to Clay Colloid Chemistry. – N. Y.: Interscience Publishers, 1983.
22. *Bergaya F., Vayer M.* // Applied Clay Science. – 1997. – **12**. – P. 275.
23. *Boissay Sylvie.* Comparaison des méthodes de détermination des points de charge nulle. Thesis, Département Minéralurgie du Bureau de Recherche Géologique et Minières à Orléans, France, 1984.
24. *Duc M., Gaboriaud F., Thomas F.* // J. Coll. Interf. Sci. – 2005. – **289**. – P. 148.
25. *Schroth B.L., Sposito G.* // Clays Clay Miner. – 1997. – **45**. – P. 85.
26. *Srasra E., Bergaya F., Fripiat J.J.* // Ibid. – 1994. – **42**. – P. 237.

27. *Parks G.A.* // Chem. Reviews. – 1965. – **65**. – P. 177.
28. *Mustapha S., Dilara B., Nargis K. et al*. // Coll. Surf. A. – 2002. – **205**. – P. 273.
29. *Kosmulski M.J.* // Coll. Interf. Sci. – 2006. – **298**. – P. 730.
30. *Wieland E., Stumm W.* // Geochim. Cosmochim. Acta. – 1992. – **56**. – P. 3339.
31. *Huertas J.F., Chou L., Wollast R.* // Ibid. – 1998. – **62**. – P. 417.
32. *Hayes K.F., Redden G., Ela W., Leckie J.O.* // J. Coll. Interf. Sci. – 1991. – **142**. – P. 2.
33. *Jolivet J.P.* De la solution à l′oxyde. Condensation des cations en solution aqueuse, Chimie de Surface des Oxydes. Editeur: EDP Sciences. ISBN: 2-86883-371-3, 1998.
34. *De Faria L.A., Trassati S.* // J. Electroanalytical Chem. – 2003. – **554-555**. – P. 355 – 359.
35. *Lu W., Smith E.H.* // Geochim. Cosmochim. Acta. – 1996. – **60**. – P. 3363.
36. *Motta M.M., Miranda C.F.* // Soil Sci. Soc. Amer. J. – 1989. – **53**. – P. 380.
37. *Boclair J.W., Braterman P.S.* // Chem. Mater. – 1999. – **11**. – P. 298.
38. *Davis J.A., Leckie J.O. Russ.* // J. Coll. Interf. Sci. – 1978. – **67**. – P. 90.
39. *Sverjensky D.* // Geochim. Cosmochim. Acta. – 2005. – **69**. – P. 225.
40. *Sprycha R.* // J. Coll. Interf. Sci. – 1989. – **127**. – P. 1.
41. *Tombacz E., Szekeres M., Kertesz I., Turi L.* // Prog. Colloid & Polym. Sci. – 1995. – **98**. – P. 160.
42. *Kummert R., Stumm W.* // J. Coll. Interf. Sci. – 1980. – **75**. – P. 373.
43. *Kriaa A., Hamdi N., Srasra E.* // Russ. J. Electrochem. – 2007. – **43**. – P 167.